Constraints on the coupling between Dark Matter and Dark Energy from CMB data

Riccardo Murgia (SISSA, Trieste)

Università degli Studi di Cagliari May 2016

Outline

- Cosmic Microwave Background anisotropies
  - Temperature power spectrum
  - Polarization
  - Cosmological parameters estimation
- Coupling between Dark Matter and Dark Energy
  - Theoretical model and parameterization
  - Data analysis method
- Results

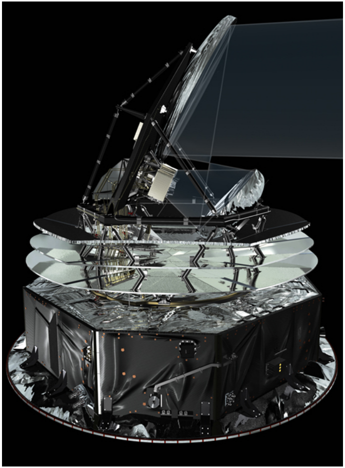

Cosmic Microwave Background (CMB)

More than 20 years of CMB experiments...

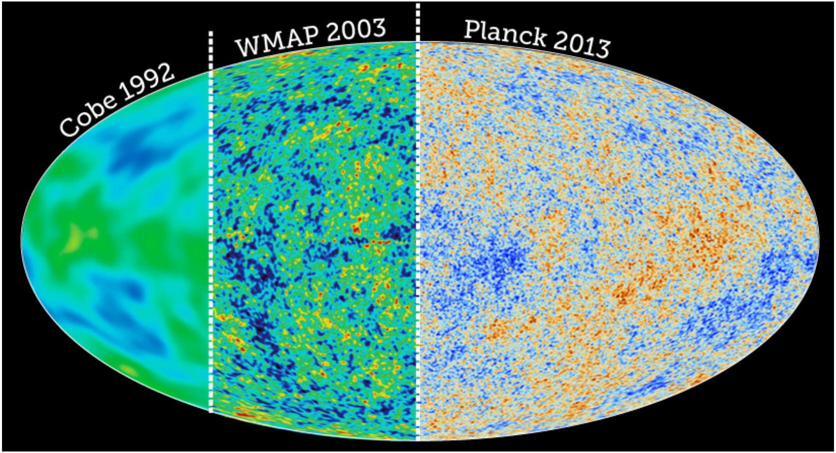

Angular power spectrum

Temperature field of Universe: $T(\vec{x}, \hat{p}, \eta) = T(\eta)(1 + \Theta(\vec{x}, \hat{p}, \eta))$

Spherical harmonics expansion: $\Theta(\vec{x}, \hat{p}, \eta) = \sum_{l=1}^{\infty} \sum_{m=-l}^{l} \Theta_{lm}(\vec{x}, \eta) Y_{lm}(\hat{p})$

Angular power spectrum: $< \Theta_{lm} \Theta^*_{l'm'} >= \delta_{ll'} \delta_{mm'} C_l^{TT}$

$\Theta \equiv \frac{\delta T}{T}$; $\eta \equiv \int_0^t \frac{dt'}{a(t')}$; $\hat{p} \rightarrow$ photon direction; $Y_{lm}(\hat{p}) \rightarrow$ spherical harmonics

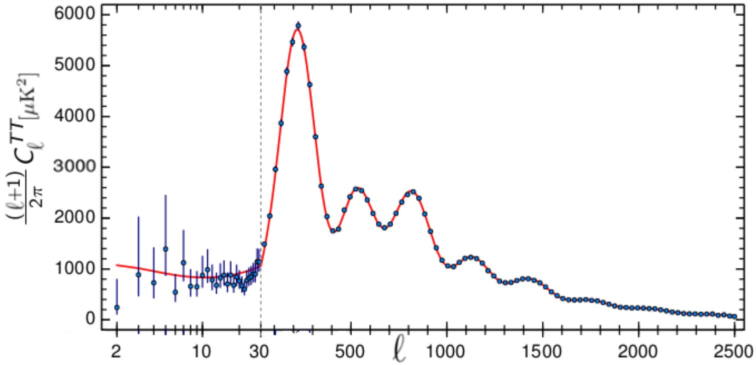

[Planck Collaboration - 2015]

Polarization

Linear polarization tensor:

$$P_{ij} \propto \begin{pmatrix} \Theta + Q & U \\ -U & \Theta - Q \end{pmatrix}$$

Harmonic expansion:

$$Q(\hat{p}) \pm iU(\hat{p}) = \sum_{l=1}^{\infty} \sum_{m=-l}^{l} (E_{lm} \pm iB_{lm})_{\pm 2}Y_{lm}(\hat{p})$$

Non-vanishing polarization power spectra:

$$\begin{aligned} < E_{lm}E^*_{l'm'} > &= \delta_{ll'}\delta_{mm'}C_l^{EE} \\ < B_{lm}B^*_{l'm'} > &= \delta_{ll'}\delta_{mm'}C_l^{BB} \\ < \Theta_{lm}E^*_{l'm'} > &= \delta_{ll'}\delta_{mm'}C_l^{TE} \end{aligned}$$

$\Theta \equiv \frac{\delta T}{T}$; $\hat{p} \rightarrow$ photon direction; ${}_{\pm 2}Y_{lm}(\hat{p}) \rightarrow$ spherical harmonics; Q,U $\rightarrow$ Stokes parameters

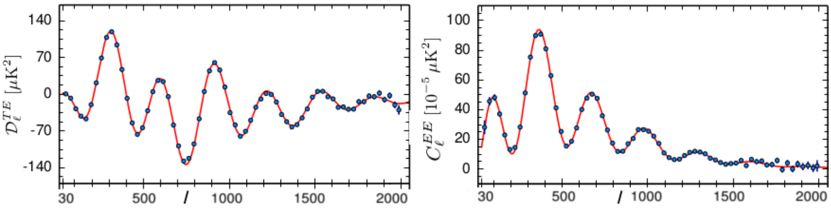

[Planck Collaboration - 2015]

Cosmological parameters estimation

$$\Omega_i \equiv \frac{8\pi G \rho_i}{3H^2}$$

$$\Omega_k \equiv 1 - \Omega_m - \Omega_\Lambda = 0.000 \pm 0.005$$

(95% C.L. Planck+lensing+BAO) [a]

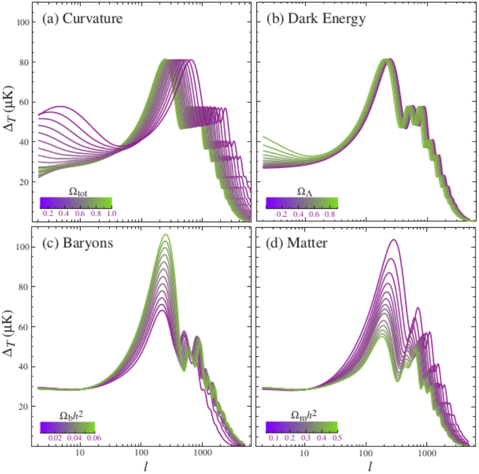

[Hu and Dodelson - 2002]

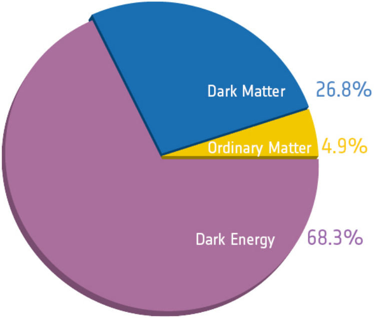

[a] [Planck Collaboration - 2015]

Coupling between Dark Matter (DM) and Dark Energy (DE)

R. Murgia[a,b,c] **S. Gariazzo**[a,b] **N. Fornengo**[a,b]

[a]Department of Physics, University of Torino, Via P. Giuria 1, I–10125 Torino, Italy
[b]INFN, Sezione di Torino, Via P. Giuria 1, I–10125 Torino, Italy
[c]SISSA/ISAS, International School for Advanced Studies, via Bonomea 265, 34136 Trieste, Italy

E-mail: riccardo.murgia@sissa.it, gariazzo@to.infn.it, fornengo@to.infn.it

Abstract. We investigate a phenomenological non-gravitational coupling between dark energy and dark matter, where the interaction in the dark sector is parameterized as an energy transfer either from dark matter to dark energy or the opposite. The models are constrained by a whole host of updated cosmological data: cosmic microwave background temperature anisotropies and polarization, high-redshift supernovae, baryon acoustic oscillations, redshift space distortions and gravitational lensing. Both models are found to be compatible with all cosmological observables, but in the case where dark matter decays into dark energy, the tension with the independent determinations of H_0 and σ_8, already present for standard cosmology, increases: this model in fact predicts lower H_0 and higher σ_8, mostly as a consequence of the higher amount of dark matter at early times, leading to a stronger clustering during the evolution. Instead, when dark matter is fed by dark energy, the reconstructed values of H_0 and σ_8 nicely agree with their local determinations, with a full reconciliation between high- and low-redshift observations. A non-zero coupling between dark energy and dark matter, with an energy flow from the former to the latter, appears therefore to be in better agreement with cosmological data.

JCAP 04 (2016) 14 arXiv:1602.01765

Coupling between Dark Matter (DM) and Dark Energy (DE)

A choice among many phenomenological interaction models: $Q = \mathcal{H}\xi\rho_\Lambda$ [1] [2]

$\mathcal{H} = \frac{\dot{a}}{a} \equiv \frac{1}{a}\frac{da}{d\eta}$; $\xi \rightarrow$ dimensionless coupling parameter; $\rho_\Lambda \rightarrow$ DE energy density

Background evolution in the presence of coupling:

$$\dot{\rho}_\Lambda + 3\mathcal{H}(1 + w_\Lambda)\rho_\Lambda = 0 \longrightarrow \dot{\rho}_\Lambda + 3\mathcal{H}(1 + w_\Lambda)\rho_\Lambda = -Q$$

$$\dot{\rho}_{DM} + 3\mathcal{H}\rho_{DM} = 0 \longrightarrow \dot{\rho}_{DM} + 3\mathcal{H}\rho_{DM} = +Q$$

Q < 0 ($\xi < 0$) $\Rightarrow$ Energy flux from DM to DE, i.e. DM decays into DE (**MOD1**)

Q > 0 ($\xi > 0$) $\Rightarrow$ Energy flux from DE to DM, i.e. DE decays into DM (**MOD2**)

[1] [Salvatelli et al. - 2013]
[2] [Costa et al. - 2014]

Data analysis method

- **Computing the CMB power spectrum**
  Modified version of the numerical Boltzmann solver CAMB [3], in which we have included:
  - Background equations in the presence of DE-DM coupling

$$\begin{aligned}\rho_\Lambda &= \rho_{\Lambda_0} a^{-3(w_\Lambda+1)-\xi} \\ \rho_{DM} &= \rho_{DM_0} a^{-3} + \rho_{\Lambda_0} a^{-3}\left[\frac{\xi}{3w_\Lambda+\xi}\left(1-a^{3w_\Lambda-\xi}\right)\right]\end{aligned}$$

  - Linear perturbations equations in the presence of DE-DM coupling, in the synchronous gauge ($h = 6\Phi$; $\delta \equiv \frac{\delta\rho_i}{\rho_i}$)

$$\begin{aligned}\dot{\delta}_\Lambda &= -(1+w_\Lambda)\left(kv_\Lambda + \frac{\dot{h}}{2}\right) - 3\mathcal{H}(1-w_\Lambda)\left(\delta_\Lambda \mathcal{H}(3(1+w_\Lambda)+\xi)\frac{v_\Lambda}{k}\right) \\ \dot{v}_\Lambda &= -2\mathcal{H}\left(1+\frac{\xi}{1+w_\Lambda}\right)v_\Lambda + k\frac{\delta_\Lambda}{1+w_\Lambda} \\ \dot{\delta}_{DM} &= -\left(kv_{DM}+\frac{\dot{h}}{2}\right) + \xi\mathcal{H}\frac{\rho_\Lambda}{\rho_{DM}}(\delta_\Lambda - \delta_{DM}) \\ \dot{v}_{DM} &= -\mathcal{H}v_{DM}\left(1+\xi\frac{\rho_\Lambda}{\rho_{DM}}\right)\end{aligned}$$

- **Comparing theory with observations**
  Slightly adjusted version of the Markov Chain Monte Carlo (MCMC) code CosmoMC [4], in order to include ξ as an additional free parameter.

---

[3] http://camb.info/

[4] http://cosmologist.info/cosmomc/

Datasets for the analysis

- **CMB**: combination of the the high-ℓ ($2 \leq \ell \leq 2500$) TT spectrum with the low-ℓ ($2 \leq \ell \leq 29$) polarization spectra ("PlanckTT+lowP") by Planck, plus the high-ℓ ($2 \leq \ell \leq 2500$) polarization spectra ("highP") and the power spectrum of the lensing potential ("lens") by Planck [Planck Collaboration - 2015]
- **BAO/RSD**:Baryon Acoustic Oscillations (BAO) measurements from 6dF Galaxy Survey at z=0.106 [Beutler et al. - 2011], SDSS DR7 MGS at z=0.15 [Ross et al. - 2015], BOSS DR11 at z=0.32 [BOSS Collaboration - 2014], combined with Redshift Space Distortions (RSD) data from BOSS CMASS DR11 at z=0.57 [Samushia et al. - 2014]
- **JLA**: SNIa data from the Joint Light-curve Analysis ("JLA") of more than 740 samples of SNIa from z=0.02 to z=1.3 [Betoule et al. - 2014], including Hubble Space Telescope (HST) results [Riess et al. - 2011]

$H_0 \rightarrow$ current Hubble expansion rate; $\sigma_8 \rightarrow$ current root mean square linear matter fluctuation in a $8h^{-1}$ Mpc sphere

Datasets for the analysis

- **CMB**: combination of the the high-ℓ ($2 \leq \ell \leq 2500$) TT spectrum with the low-ℓ ($2 \leq \ell \leq 29$) polarization spectra ("PlanckTT+lowP") by Planck, plus the high-ℓ ($2 \leq \ell \leq 2500$) polarization spectra ("highP") and the power spectrum of the lensing potential ("lens") by Planck [Planck Collaboration - 2015]
- **BAO/RSD**:Baryon Acoustic Oscillations (BAO) measurements from 6dF Galaxy Survey at z=0.106 [Beutler et al. - 2011], SDSS DR7 MGS at z=0.15 [Ross et al. - 2015], BOSS DR11 at z=0.32 [BOSS Collaboration - 2014], combined with Redshift Space Distortions (RSD) data from BOSS CMASS DR11 at z=0.57 [Samushia et al. - 2014]
- **JLA**: SNIa data from the Joint Light-curve Analysis ("JLA") of more than 740 samples of SNIa from z=0.02 to z=1.3 [Betoule et al. - 2014], including Hubble Space Telescope (HST) results [Riess et al. - 2011]

Tensions between local and CMB measurements, assuming ΛCDM:

- **HST**: 68% constraints on H_0 from HST low-redshift measurements [Riess et al. - 2011]:

  $H_0 = 73.8 \pm 2.4$ km s^{-1}Mpc^{-1}

  $H_0 = 70.6 \pm 3.3$ km s^{-1}Mpc^{-1} ("GE") [Efstathiou - 2013]
- **WL**: 68% constraints on σ_8 from CFHTLenS Weak Lensing (WL) data:

  $\sigma_8 = 0.774^{+0.032}_{-0.041}$ [Heymans et al. - 2013]
- **SZ**: 68% constraints on σ_8 from Planck Sunyaev-Zel'dovich ("SZ") cluster counts:

  $\sigma_8 = 0.75 \pm 0.03$ [Planck Collaboration - 2015]

- 68% constraints from CMB data, assuming ΛCDM ("PlanckTT+lowP") [Planck Collaboration - 2015]:

  $H_0 = 67.3 \pm 1.0$ km s^{-1}Mpc^{-1}

  $\sigma_8 = 0.828 \pm 0.012$

UNEXPLAINED DISCREPANCIES AT MORE THAN 2σ!

$H_0 \rightarrow$ current Hubble expansion rate; $\sigma_8 \rightarrow$ current root mean square linear matter fluctuation in a $8h^{-1}$ Mpc sphere

Priors choice

For the MCMC analysis, we adopted flat priors in the listed intervals:

Parameter	Prior	
$\Omega_b h^2$	[0.005, 0.1]	
$\Omega_c h^2$	[0.001, 0.5]	
100θ	[0.5, 10]	
τ	[0.01, 0.8]	
$\log(10^{10} A_s)$	[2.7, 4]	
n_s	[0.9, 1.1]	
	MOD1	MOD2
w_Λ	[-0.999, -0.1]	[-2.5, -1.001]
ξ	[-1, 0]	[0, 0.5]
$\sum m_\nu$	0.06 eV	
N_ν	3.046	

$\Omega_b h^2 \rightarrow$ current baryonic abundance

$\Omega_c h^2 \rightarrow$ current CDM abundance

$\theta \rightarrow$ ratio of the sound horizon to the angular diameter distance at decoupling

$\tau \rightarrow$ optical depth at reionization

$n_s \rightarrow$ scalar spectral index at $k = 0.05$ Mpc^{-1}

$A_s \rightarrow$ primordial scalar perturbation spectrum amplitude at $k = 0.05$ Mpc^{-1}

$w_\Lambda \rightarrow$ DE equation of state

$\xi \rightarrow$ coupling parameter

$\sum m_\nu \rightarrow$ total neutrino mass

$N_\nu \rightarrow$ effective number of neutrinos

Effects on the TT power spectrum

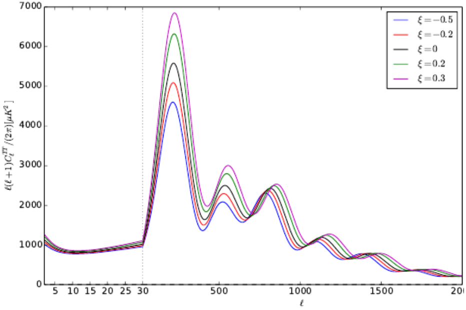

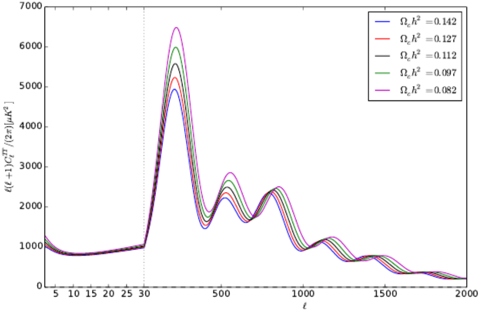

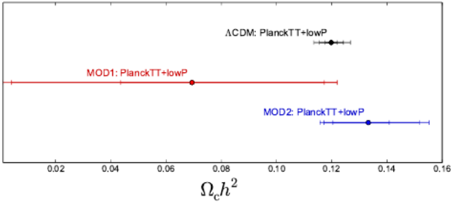

Results

2σ constraints with "PlanckTT+lowP" dataset:

Parameter	ΛCDM	MOD1	MOD2
$100\Omega_b h^2$	$2.222^{+0.047}_{-0.043}$	$2.216^{+0.046}_{-0.045}$	$2.226^{+0.047}_{-0.046}$
$\Omega_c h^2$	$0.120^{+0.004}_{-0.004}$	$0.069^{+0.053}_{-0.065}$	$0.133^{+0.019}_{-0.016}$
100θ	$1.0409^{+0.0009}_{-0.0009}$	$1.0441^{+0.0052}_{-0.0040}$	$1.0402^{+0.0013}_{-0.0013}$
τ	$0.078^{+0.039}_{-0.037}$	$0.077^{+0.039}_{-0.038}$	$0.077^{+0.039}_{-0.038}$
n_s	$0.965^{+0.012}_{-0.012}$	$0.964^{+0.013}_{-0.012}$	$0.966^{+0.013}_{-0.012}$
$\log(10^{10}A_s)$	$3.089^{+0.074}_{-0.072}$	$3.088^{+0.073}_{-0.073}$	$3.087^{+0.073}_{-0.074}$
ξ	0	$(-0.789, 0]$	$[0, 0.269)$
w_Λ	-1	$[-1, -0.703)$	$-1.543^{+0.524}_{-0.447}$
H_0 [Km s^{-1} Mpc^{-1}]	$67.28^{+1.92}_{-1.89}$	$67.91^{+7.44}_{-7.87}$	> 68.32
σ_8	$0.830^{+0.029}_{-0.028}$	$1.464^{+1.948}_{-1.037}$	$0.898^{+0.163}_{-0.160}$

Bounds on ξ in **MOD1**:

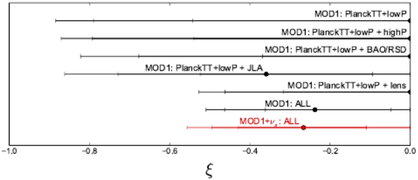

2σ constraints with "ALL" dataset:

Parameter	ΛCDM	MOD1	MOD2
$100\Omega_b h^2$	$2.229^{+0.028}_{-0.028}$	$2.228^{+0.030}_{-0.030}$	$2.227^{+0.031}_{-0.030}$
$\Omega_c h^2$	$0.119^{+0.002}_{-0.002}$	$0.091^{+0.029}_{-0.033}$	$0.135^{+0.014}_{-0.014}$
100θ	$1.0409^{+0.0006}_{-0.0006}$	$1.0426^{+0.0022}_{-0.0019}$	$1.0400^{+0.0010}_{-0.0010}$
τ	$0.062^{+0.025}_{-0.025}$	$0.063^{+0.027}_{-0.026}$	$0.059^{+0.028}_{-0.027}$
n_s	$0.966^{+0.008}_{-0.008}$	$0.966^{+0.009}_{-0.009}$	$0.966^{+0.009}_{-0.009}$
$\log(10^{10}A_s)$	$3.055^{+0.045}_{-0.046}$	$3.058^{+0.049}_{-0.049}$	$3.050^{+0.050}_{-0.051}$
ξ	0	$(-0.463, 0]$	$[0, 0.300)$
w_Λ	-1	$[-1, -0.829)$	$(-1.129, -1]$
H_0 [Km s^{-1} Mpc^{-1}]	$67.72^{+1.01}_{-0.97}$	$67.57^{+1.81}_{-1.79}$	$67.83^{+1.90}_{-1.75}$
σ_8	$0.812^{+0.017}_{-0.017}$	$0.994^{+0.294}_{-0.219}$	$0.749^{+0.069}_{-0.063}$

Bounds on ξ in **MOD2**:

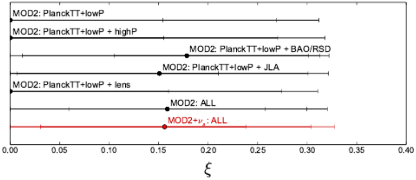

Results

2σ constraints with "PlanckTT+lowP" dataset:

Parameter	ΛCDM	MOD1	MOD2
$100\Omega_b h^2$	$2.222^{+0.047}_{-0.043}$	$2.216^{+0.046}_{-0.045}$	$2.226^{+0.047}_{-0.046}$
$\Omega_c h^2$	$0.120^{+0.004}_{-0.004}$	$0.069^{+0.053}_{-0.065}$	$0.133^{+0.019}_{-0.016}$
100θ	$1.0409^{+0.0009}_{-0.0009}$	$1.0441^{+0.0052}_{-0.0040}$	$1.0402^{+0.0013}_{-0.0013}$
τ	$0.078^{+0.039}_{-0.037}$	$0.077^{+0.039}_{-0.038}$	$0.077^{+0.039}_{-0.038}$
n_s	$0.965^{+0.012}_{-0.012}$	$0.964^{+0.013}_{-0.012}$	$0.966^{+0.013}_{-0.012}$
$\log(10^{10}A_s)$	$3.089^{+0.074}_{-0.072}$	$3.088^{+0.073}_{-0.073}$	$3.087^{+0.073}_{-0.074}$
ξ	0	$(-0.789, 0]$	$[0, 0.269)$
w_Λ	-1	$[-1, -0.703)$	$-1.543^{+0.524}_{-0.447}$
H_0 [Km s^{-1} Mpc^{-1}]	$67.28^{+1.92}_{-1.89}$	$67.91^{+7.44}_{-7.87}$	> 68.32
σ_8	$0.830^{+0.029}_{-0.028}$	$1.464^{+1.948}_{-1.037}$	$0.898^{+0.163}_{-0.160}$

2σ constraints with "ALL" dataset:

Parameter	ΛCDM	MOD1	MOD2
$100\Omega_b h^2$	$2.229^{+0.028}_{-0.028}$	$2.228^{+0.030}_{-0.030}$	$2.227^{+0.031}_{-0.030}$
$\Omega_c h^2$	$0.119^{+0.002}_{-0.002}$	$0.091^{+0.029}_{-0.033}$	$0.135^{+0.014}_{-0.014}$
100θ	$1.0409^{+0.0006}_{-0.0006}$	$1.0426^{+0.0022}_{-0.0019}$	$1.0400^{+0.0010}_{-0.0010}$
τ	$0.062^{+0.025}_{-0.025}$	$0.063^{+0.027}_{-0.026}$	$0.059^{+0.028}_{-0.027}$
n_s	$0.966^{+0.008}_{-0.008}$	$0.966^{+0.009}_{-0.009}$	$0.966^{+0.009}_{-0.009}$
$\log(10^{10}A_s)$	$3.055^{+0.045}_{-0.046}$	$3.058^{+0.049}_{-0.049}$	$3.050^{+0.050}_{-0.051}$
ξ	0	$(-0.463, 0]$	$[0, 0.300)$
w_Λ	-1	$[-1, -0.829)$	$(-1.129, -1]$
H_0 [Km s^{-1} Mpc^{-1}]	$67.72^{+1.01}_{-0.97}$	$67.57^{+1.81}_{-1.79}$	$67.83^{+1.90}_{-1.75}$
σ_8	$0.812^{+0.017}_{-0.017}$	$0.994^{+0.294}_{-0.219}$	$0.749^{+0.069}_{-0.063}$

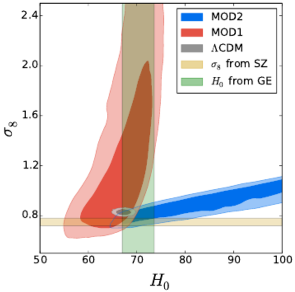

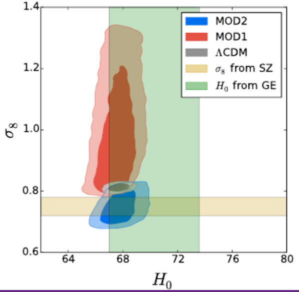

Sterile neutrino as stable DM component

	Prior	
Parameter	ΛCDM	ν_s
$m_s^{\rm eff}(eV)$	0	[0,15]
$N_{\rm eff}$	3.046	[3.046, 6]

Table 5. Priors on the neutrino parameters $m_s^{\rm eff}$ and $N_{\rm eff}$. The priors are assumed flat.

$m_s^{\rm eff} = (94.1\mathrm{eV})\,\Omega_s h^2 \rightarrow$ effective sterile neutrino mass

$N_{\rm eff} \rightarrow$ effective number of neutrinos

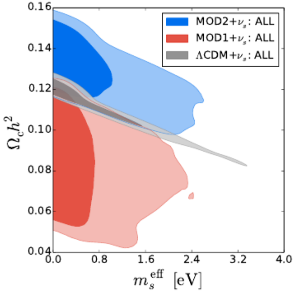

2σ constraints with "ALL" dataset:

Parameter	ΛCDM	MOD1	MOD2
$100\Omega_b h^2$	$2.237^{+0.034}_{-0.031}$	$2.237^{+0.036}_{-0.032}$	$2.236^{+0.035}_{-0.032}$
$\Omega_c h^2$	$0.113^{+0.014}_{-0.019}$	$0.083^{+0.034}_{-0.033}$	$0.129^{+0.024}_{-0.025}$
100θ	$1.0408^{+0.0006}_{-0.0007}$	$1.0426^{+0.0022}_{-0.0020}$	$1.0400^{+0.0010}_{-0.0011}$
τ	$0.063^{+0.032}_{-0.033}$	$0.064^{+0.034}_{-0.035}$	$0.060^{+0.034}_{-0.035}$
n_s	$0.969^{+0.012}_{-0.011}$	$0.968^{+0.013}_{-0.012}$	$0.968^{+0.012}_{-0.012}$
$\log(10^{10}A_s)$	$3.059^{+0.066}_{-0.067}$	$3.061^{+0.068}_{-0.070}$	$3.054^{+0.070}_{-0.069}$
ξ	0	$(-0.494, 0]$	$[0, 0.304)$
w_Λ	-1	$[-1, -0.841)$	$(-1.162, -1]$
$m_s^{\rm eff}$ [eV]	< 2.1	< 1.9	< 2.2
$N_{\rm eff}$	< 3.34	< 3.38	< 3.35
H_0 [Km s^{-1} Mpc^{-1}]	$67.91^{+1.33}_{-1.26}$	$68.23^{+2.21}_{-2.00}$	$68.43^{+2.16}_{-2.07}$
σ_8	$0.789^{+0.039}_{-0.045}$	$0.988^{+0.300}_{-0.229}$	$0.727^{+0.073}_{-0.072}$

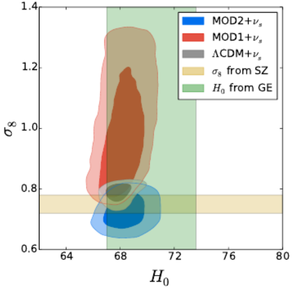

GrAtziAs medA

po s'Attentzioni!

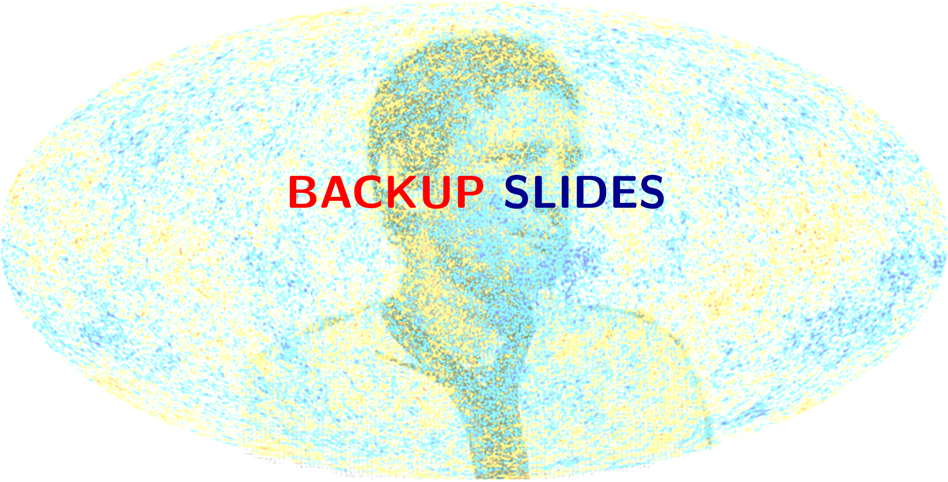

BACKUP SLIDES

DE phantom behaviour

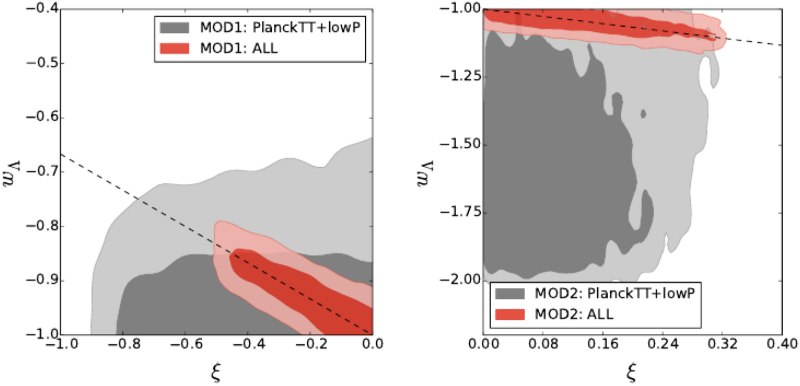

Figure 5. Marginalized 1σ and 2σ C.L. allowed regions in the $(\xi,\, w_\Lambda)$ plane in MOD1 (left) and MOD2 (right), for different datasets. The dashed line makes the area below the dashed lines ($w_\Lambda^{\rm eff} = w_\Lambda + \xi/3 = -1$) corresponds to an increasing energy density for DE in the future.

Data analysis method

- **CAMB**[5] : Code for Anisotropies in the Microwave Background.
  Numerically solves the Boltzmann equations in linear perturbation theory and, given a cosmological model, generates predictions for the observables.
- **CosmoMC**[6] : Markov-Chain Monte-Carlo (MCMC) engine for exploring cosmological parameter space.
  It takes as inputs the parameter prior distribution functions $P(\mathcal{I})$ and uses data and likelihoods $P(d|\mathcal{I})$ to find the best fit model, through Bayesian inference:

$$P(\mathcal{I}|d) = \frac{P(d|\mathcal{I})P(\mathcal{I})}{P(d)}$$

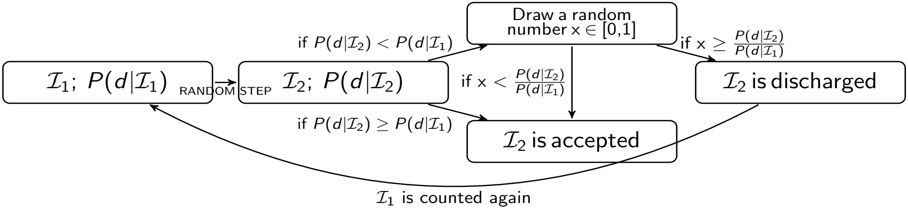

density of sampled points $\propto$ posterior distribution

$\mathcal{I}_1$, $\mathcal{I}_2$ $\rightarrow$ random points in the parameter space (*Metropolis-Hastings* algorithm)

[5] http://camb.info/
[6] http://cosmologist.info/cosmomc/